Comparative Analysis of the Far Lateral, Far Medial, and Contralateral Transmaxillary Approaches to the Jugular Tubercle

Cleiton Formentin, MD, PhD [*‡], **Arseniy Pichugin, MD, PhD** [*§], **Yun-Kai Chan, MD** [*‖], **Albert Trondin, MD** [¶], **Georgios A. Zenonos, MD** [*], **Eric W. Wang, MD** [#], **Carl H. Snyderman, MD, MBA** [#], **Paul A. Gardner, MD** [*]

*Department of Neurological Surgery, University of Pittsburgh School of Medicine, Pittsburgh, Pennsylvania, USA; ‡Department of Neurology, University of Campinas, São Paulo, Brazil; §Department of Neurological Surgery, Kazan State Medical University, Kazan, Russia; ‖Department of Neurological Surgery, MacKay Memorial Hospital, Taipei, Taiwan; ¶Department of Neurological Surgery, Hospital Clínico San Carlos, Madrid, Spain; #Department of Otolaryngology, University of Pittsburgh School of Medicine, Pittsburgh, Pennsylvania, USA

Presented as an On-Demand abstract at the North American Skull Base Society (NASBS) 2021 online meeting, February 13, 2021.

Correspondence: Paul A. Gardner, MD, Department of Neurological Surgery, University of Pittsburgh, UPMC Presbyterian, Suite B-400, 200 Lothrop St, Pittsburgh, PA 15213, USA. Email: gardpa@upmc.edu Cleiton Formentin, MD, PhD, Department of Neurological Surgery, University of Pittsburgh, UPMC Presbyterian, Suite B-400, 200 Lothrop St, Pittsburgh, PA 15213, USA. Email: cleitonformentin@gmail.com

Received, April 19, 2025; **Accepted,** August 12, 2025; **Published Online,** October 15, 2025.

Operative Neurosurgery 00:1–13, 2025 https://doi.org/10.1227/ons.0000000000001804

BACKGROUND AND OBJECTIVES: The jugular tubercle (JT) is a bony prominence located between the basilar and condylar parts of the occipital bone, superior to the hypoglossal canal. This study compares the volume of the JT removed, the overall area of exposure and the surgical corridor among the far lateral approach (FLA), far medial approach (FMA), and contralateral transmaxillary (CTM) corridor.

METHODS: Using image guidance, 10 cadaveric specimens were dissected: The JT was drilled through FMA and CTM in 10 sides, whereas FLA was performed on the opposite 10 sides. The surgical corridor and overall area of exposure were measured. A subanalysis was conducted to compare the angle of the surgical trajectory between FMA and CTM. Computed tomography scan volumetric measurements were used to compare the approaches. Five illustrative cases are presented.

RESULTS: The angle of the surgical trajectory to the JT was significantly greater for CTM (33.8° ± 7.1°) compared with FMA (14.3° ± 2.6°, $P < .001$). The area of exposure was significantly larger with FLA (410.7 ± 78.1 mm^2) and CTM (436.8 ± 44.8 mm^2) compared with FMA (270.7 ± 21.9 mm^2, $P < .001$). In addition, CTM (212.2 ± 32.2 mm^2) provided a significantly wider surgical corridor than FMA (82.7 ± 12.4 mm^2, $P < .001$) and showed a trend toward greater exposure compared with FLA ($P = .05$). The mean percentage of JT resected was 56.7% for FLA, 40.4% for FMA, and 94% for CTM ($P < .05$).

CONCLUSION: Open and endoscopic approaches are complementary for addressing lesions in the inferior clival and petroclival regions. The CTM approach represents a feasible extension of the standard endoscopic endonasal approach, increasing the surgical corridor angle and providing greater lateral exposure than the FMA. In addition, CTM enables a substantially greater volume of JT resection compared with both FLA and FMA.

KEY WORDS: Jugular tubercle, Inferior clivus, Endoscopic endonasal approach, Far medial approach, Far lateral approach, Contralateral transmaxillary corridor

The jugular tubercle (JT) is an oval bony prominence located between the basilar and condylar parts of the occipital bone, positioned just above and anterior to the hypoglossal canal, medial to the jugular foramen (JF) and between the jugular bulb and inferior petrosal sinus.[1-3] It is composed of hard compact bone, and the lower cranial nerves (CNs) cross its posterior part while passing from the brainstem to the JF (Figure 1).

To maximize surgical exposure with the far lateral approach (FLA), satisfactory removal of the JT is essential. Quantitatively, JT removal yields the most significant increase in the exposed petroclival area, enhancing visualization ventral to the brainstem and revealing the paramedullary area, vertebral artery (VA), origin of the posterior inferior cerebellar artery, and vertebrobasilar junction.[3-5] Removing this structure significantly increases the

ABBREVIATIONS: CTM, contralateral transmaxillary; **EEA,** endoscopic endonasal approach; **FLA,** far lateral approach; **FMA,** far medial approach; **IAC,** internal acoustic canal; **JF,** jugular foramen; **JT,** jugular tubercle; **VA,** vertebral artery.

Supplemental digital content is available for this article at operativeneurosurgery-online.com.

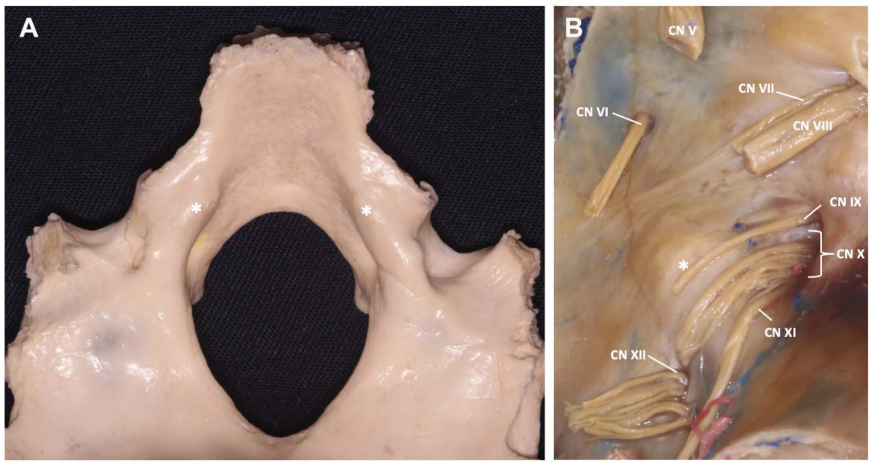

FIGURE 1. A, *The image illustrates the anatomy of the occipital bone, with particular emphasis on the JT (asterisk). The JT is located between the basilar and condylar parts of the occipital bone, situated superiorly and anteriorly to the hypoglossal canal.* **B**, *The lower CNs traverse the posterior part of the JT while passing from the brainstem to the JF. CN, cranial nerve; JF, jugular foramen; JT, jugular tubercle.*

operative field from the foramen magnum toward the clivus, providing a flat viewing angle and greater exposure of the ventrolateral brainstem.

Currently, the expanded endoscopic endonasal approach (EEA) is considered a safe and effective surgical route for tumors involving the inferior clivus.[6-9] The transjugular tubercle variant of the "far medial" endonasal approach (FMA) allows direct access to ventrolateral lesions in the inferior clival region, but significant challenges arise when access to more lateral areas, such as the JT, is needed.[1,10,11] The contralateral transmaxillary (CTM) corridor has been described as a feasible extension of the standard EEA, offering a more lateral trajectory.[12] This corridor runs more parallel to the course of the horizontal petrous internal carotid artery (ICA), allowing greater access to more lateral aspects of the petrous apex without requiring extensive manipulation of the ICA. The aim of this study was to compare the volume of drilling of the JT, brainstem exposure, and surgical corridor between the FLA, the FMA and the CTM.

METHODS

Cadaveric Specimens' Dissections

Using image guidance, 10 colored silicone-injected human head specimens (20 sides) were dissected in a neurosurgical laboratory. The use of human cadaveric specimens was approved by the Committee for Oversight to Research Involving the Dead, and appropriate permission was obtained for the publication of the cadaveric images. Institutional Review Board/ethics committee approval were neither required nor sought for this study. In all clinical cases, patients provided informed consent to undergo the procedure. Predissection computed tomography [CT] scans were performed and uploaded into a neuronavigation system (Stryker).

On 10 sides, FMA and CTM approaches were performed endoscopically (Hopkins II, Karl Storz; 4 mm, 18 cm, 0°, 30°, 45°), with FMA preceding CTM. The contralateral 10 sides underwent FLA under a surgical microscope (OPMI, Zeiss; 3-40×), with images captured digitally (Canon). After JT drilling by FMA, indirect volumetric measurements using neuronavigation stereotactic points were obtained for comparison. After completing the CTM and FLA, a CT scan was performed to measure the remaining JT volume.

Far Lateral Transtubercular Approach

The JT was drilled through the FLA on 10 sides, with each cadaver head secured in a head holder. The procedure began with a curvilinear incision, followed by elevation of the musculocutaneous flap and identification of the suboccipital triangle. Dissecting laterally to medially, the VA was identified behind the atlanto-occipital joint. The extradural phase involved a suboccipital craniotomy, identification of the occipital condyle, and hemilaminectomy of the atlas. When applied to purely extradural lesions, varying degrees of mastoidectomy may be required.

The dura was opened for stereotactic measurements before drilling the JT. Extradural removal of two-thirds of the posterolateral and one-third of the posteromedial condyle provided greater exposure of the ventral brainstem.[5,13-15] To preserve atlanto-occipital joint stability, condylectomy was limited anteriorly by skeletonization of the hypoglossal canal and inferiorly by the atlas's articular facet. After this, the bone of the JT was removed extradurally, just anterior to the lower CNs.[16,17] As the drilling proceeded, bone was removed from below the cisternal segment of the accessory and vagus nerves that course above the tubercle just inside the dura.[4] After extensive bone work, additional stereotactic measurements were performed (Figure 2).

"Far Medial" Expanded Endonasal Approach

The FMA is a coronal extension of the standard EEA to the inferior clivus.[10,11] After the conventional inferior clivectomy, lateral extension

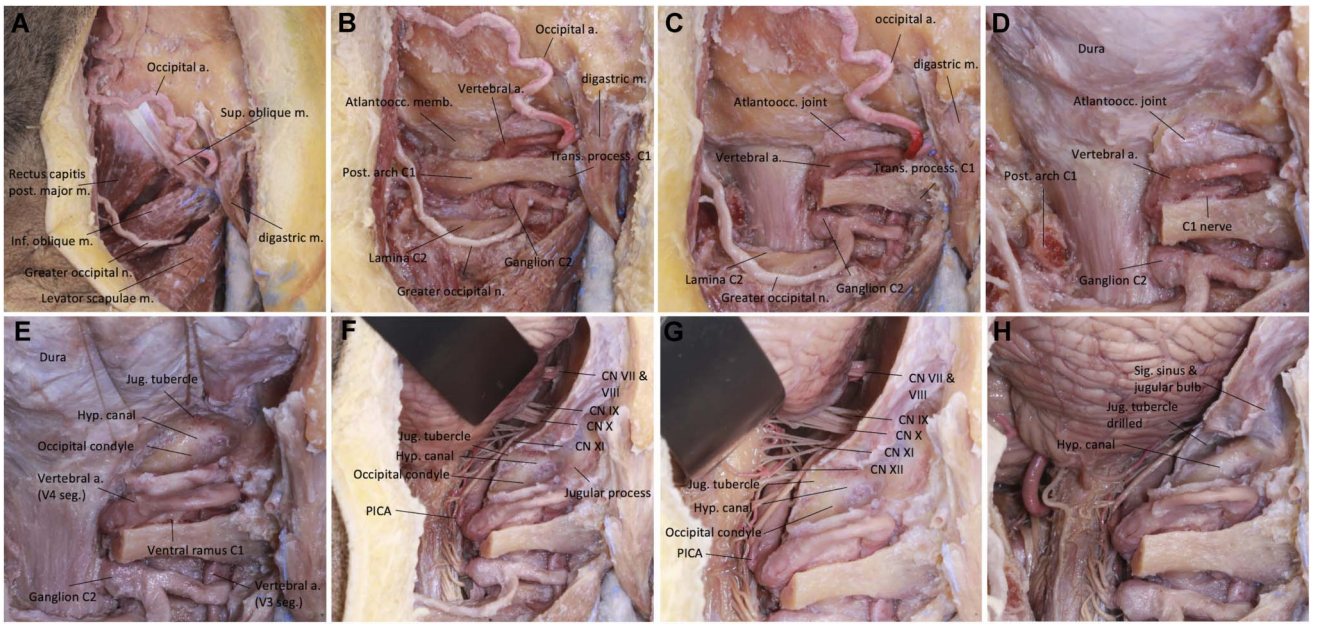

FIGURE 2. *Stepwise dissection of the far lateral transtubercular approach, right side—cadaveric pictures showing muscular dissection, extradural dissection, and intradural exposure.* **A**, *After a C-shaped incision and dissection of the superficial muscular layer, the suboccipital triangle was exposed, which is limited superiorly and medially by the rectus capitis posterior major, superiorly and laterally by the superior oblique, and inferiorly by the inferior oblique muscles; the posterior belly of the digastric muscle is attached medial to the mastoid tip along the mastoid notch; the occipital artery runs backward between the digastric and superior oblique muscles; the greater occipital nerve, arising from the dorsal ramus of C2, courses below and then behind the inferior oblique muscle.* **B**, *The superior and inferior oblique and rectus capitis posterior major muscles have been removed to provide a view of the posterior arch of C1 and the V4 segment of the VA running above it.* **C**, *Hemilaminectomy of the C1 was performed; the VA courses posterior to the atlanto-occipital joint and above the posterior arch of C1.* **D**, *A suboccipital craniotomy has been completed, and the atlanto-occipital joint has been exposed; C1 nerve courses backward, between the VA and the posterior arch of the atlas.* **E**, *The occipital condyle has been drilled until reaching the cortical bone surrounding the hypoglossal canal. The transition from cancellous to cortical bone confirms the arrival at the hypoglossal canal. Once the hypoglossal canal is exposed above the occipital condyle, the bone covering the JT that is located above the hypoglossal canal can be drilled to obtain additional exposure.* **F**, *The dura has been opened to allow stereotactic measurements, and the cerebellum has been elevated to expose the nerves in the CPA; the JT is located anterior to the glossopharyngeal, vagus, and accessory nerves.* **G**, *Magnified view of the intradural exposure; the hypoglossal nerve arises anterior to the olive and courses behind the VA to reach the hypoglossal canal; the JT is located above the hypoglossal canal and works as a trochlea around which the glossopharyngeal, vagus, and accessory nerves run in their passage from the brainstem to the JF; as the drilling proceeds, bone is removed from below the cisternal segment of the accessory and vagus nerves that course above the tubercle just inside the dura.* **H**, *The JT was drilled extradurally, allowing additional exposure of the basal cisterns and clivus, just anterior to the lower CN; the lateral margin of the JT is situated just medial to, and below, the medial edge of the jugular bulb. A, artery; atlantoocc, atlanto-occipital; CN, cranial nerve; CPA, cerebellopontine angle; hyp, hypoglossal; inf, inferior; JF, jugular foramen; JT, jugular tubercle; jug, jugular; m, muscle; n, nerve; PICA, posterior inferior cerebellar artery; post, posterior; seg, segment; sig, sigmoid; trans, transverse; VA, vertebral artery.*

begins with exposure of the supracondylar groove after partial removal of the atlanto-occipital joint capsule. The supracondylar groove, where the rectus capitis anterior muscle inserts, is a key landmark for estimating the hypoglossal canal's position beneath it. Drilling at this level exposes the canal's anterior wall, dividing the inferior clival region into tubercular and condylar compartments. The tubercular compartment represents the ventral aspect of the JT, with its posterior surface near the lower CNs as they travel toward the JF. Using a 45° rod-lens endoscope, extradural drilling of the JT was performed without mobilizing the Eustachian tube or ICA at the foramen lacerum. The boundaries of this maneuver were the inferior petrosal sinus superolaterally, the hypoglossal nerve caudally, foramen lacerum superiorly, and the Eustachian tube anterolaterally.[18] Subsequently, the dura was opened to enable initial stereotactic measurements (Figure 3).

CTM Approach

After completing the FMA and stereotactic measurements, we proceeded with the CTM on the same heads, ensuring equal distribution between sides (left and right), as sidedness can influence the ease and potentially the extent of access for a right-handed surgeon. The approach started with Caldwell-Luc procedure.[19-21] The anterior maxillotomy was extended to the zygomatic buttress and maxillary sinus wall laterally, the infraorbital nerve and foramen superiorly, while preserving the nasomaxillary buttress medially and avoiding disruption of the dental roots inferiorly.[12,22] A partial medial maxillectomy was performed on the side of the CTM. Typically, this involves resection of the posterior half of the inferior turbinate and the medial wall of the maxillary sinus down to the floor of the nasal cavity. Whenever feasible, the anterior portion of the inferior turbinate is preserved. The nasolacrimal duct is left intact without dissection. At this point, we used the drill to remove the remaining bone

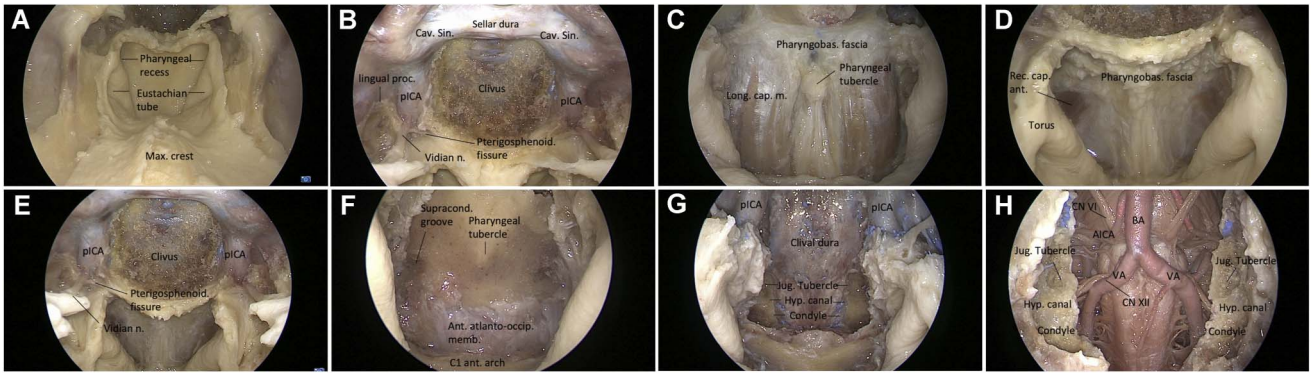

FIGURE 3. *Stepwise dissection of the far medial EEA.* **A**, *The Eustachian tube and pharyngeal recess are identified.* **B**, *The lateral recess has been exposed by a transpterygoid approach, and the floor of the sphenoid sinus has been partially drilled to expose the pharyngobasilar fascia attached to the medial aspect of the pterygosphenoidal fissure.* **C**, *Once the pharyngobasilar fascia is elevated from the inferior ventral clivus, both longus capitis muscles are exposed lateral to the pharyngeal tubercle.* **D**, *The rectus capitis anterior is a small muscle located deep to the longus capitis and attached above a small depression, the supracondylar groove.* **E**, *panoramic view.* **F**, *The pharyngeal tubercle, a consistently present bony projection at the midline, serves as a more reliable reference point for delineating the boundary between the middle and lower clivus. In addition, the supracondylar groove, situated above the occipital condyle and beneath the lateral mass of the atlas, is a key landmark for estimating the location of the hypoglossal canal and its external opening.* **G**, *After drilling the ventral inferior clivus, the underlying dura mater and basilar venous plexus are revealed. Further drilling at the lateral inferior clival area at the level of the supracondylar groove exposes the anterior cortical wall of the hypoglossal canal. This canal divides the lateral inferior clival area into 2 compartments: the tubercular (superior) and condylar (inferior). The tubercular compartment corresponds to the ventral aspect of the JT.* **H**, *Intradural anatomic structures revealed. A, artery; AICA, anterior inferior cerebellar artery; ant, anterior; atlantooccip, atlanto-occipital; BA, basilar artery; cap, capitis; cav, cavernous; CN, cranial nerve; EEA, endoscopic endonasal approach; hyp, hypoglossal; inf, inferior; JT, jugular tubercle; jug, jugular; long, longus; m, muscle; max, maxillary; memb, membrane; n, nerve; pharyngobas, pharyngobasilar; pICA, paraclival internal carotid artery; pterygosphenoid, pterygosphenoidal; rec, rectus; sigsin, sinus; supracond, supracondylar.*

above the hypoglossal canal that represents the lateral part of the JT (Figure 4).

Stereotactic Measurements

After drilling the JT, we measured the area of exposure and surgical corridor using a stereotactic navigation system. For the FLA, these measurements were taken both predrilling and postdrilling. Heron formula, based on the lengths of a triangle's sides, was used to calculate each area, and the total was obtained by summing the individual triangles. For a triangle with sides a, b, and c, the area A was calculated as: $A = \sqrt{[s(s-a)(s-b)(s-c)]}$, where s is the semiperimeter, given by $s = (a + b + c)/2$.

Surgical Corridor

The surgical corridor represents the area between neural structures that limits instrument movement within the surgical field (**Supplemental Digital Content 1, Figure 1**, http://links.lww.com/ONS/B249). We considered the following landmarks: (a) caudal-most aspect of IX rootlet (superomedial), (b) medial tip of the JT [predrilling] and entry point of IX nerve [postdrilling] (superolateral), (c) cranial-most aspect of XII rootlet (inferomedial), (d) cranial-most entry point of XII nerve into the hypoglossal canal (inferolateral), and (e) internal acoustic canal (IAC) (extreme superior and lateral point).

Overall Area of Exposure

The area of exposure was defined as the exposed surface of the brainstem and the cisternal region provided by each approach (**Supplemental Digital Content 2, Figure 2**, http://links.lww.com/ONS/B250). Dorsally, we considered the following landmarks: (a) obex (superomedial), (b) dural entry point of IX nerve (superolateral), (c) dorsal median sulcus at the C1 level (inferomedial), (d) dural entry point of the cranial-most aspect of C1 rootlet (inferolateral), and (e) IAC (extreme superior and lateral point). Ventrally: (a) pontomedullary junction (superomedial), (b) entry point of IX on JF (superolateral), (c) ventral median sulcus at C1 level (inferomedial), (d) condyle (inferolateral), and (e) IAC (extreme superior and lateral point).

Angle of Surgical Trajectory

A comparative subanalysis of FMA and CTM to the JT was conducted by evaluating the angle of surgical trajectory. After drilling the JT through the FMA, a navigation probe was advanced nasally to contact the remaining JT at multiple positions, with screen captures taken. The probe was then passed through the CTM corridor to the drilled JT. Images were analyzed in ImageJ (NIH), and the largest angle values from multiple captures were recorded for each approach.

Volumetric Assessment

After drilling the JT through the FLA and CTM, a CT scan was performed for volumetric measurements of the remaining JT, with Digital Imaging and Comunications in Medicine data imported into 3D Slicer Software (version 4.10.2 r28257, NA-NIC, NIH) for assessment.

Statistical Analysis

Statistical comparisons were performed using SPSS Statistics (version 21, IBM Corp). Depending on the data set, independent or paired t tests were applied for comparisons between approaches. A value of $P < .05$ was

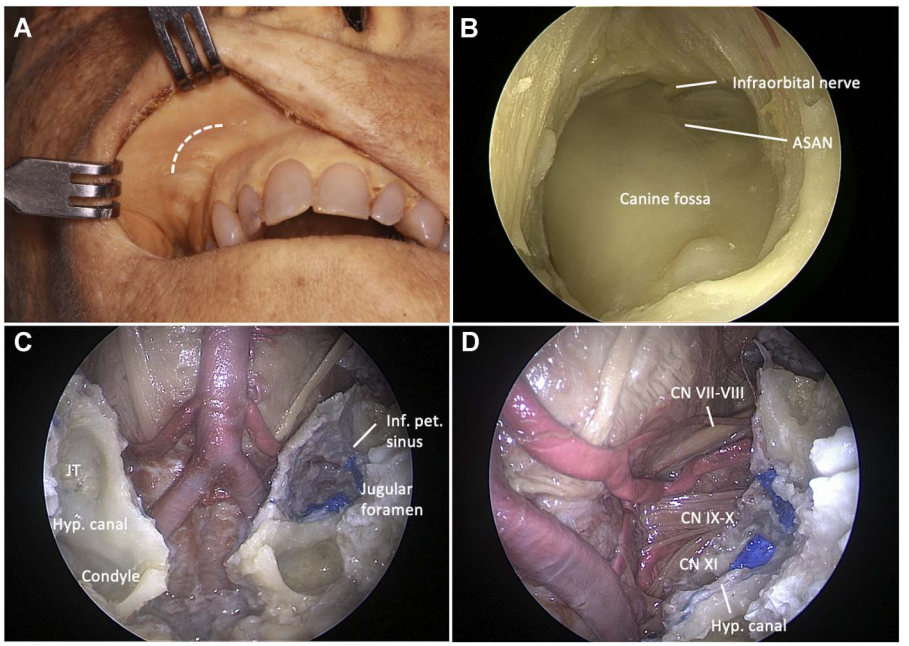

FIGURE 4. *CTM approach.* **A**, *Sublabial anterior maxillotomy (Caldwell-Luc procedure) was conducted to create an endoscopic transmaxillary corridor.* **B**, *The maxillotomy was extensively widened to the zygomatic buttress and maxillary sinus wall on the lateral side, reaching the infraorbital nerve and foramen superiorly.* **C**, *The left-sided JT was drilled out through the transmaxillary corridor.* **D**, *Intradural view. ASAN, anterior superior alveolar nerve; CN, cranial nerve; CTM, contralateral transmaxillary; hyp, hypoglossal; inf, inferior; JT, jugular tubercle; pet, petrous.*

considered statistically significant. Mean differences are reported with 95% CI.

RESULTS

Surgical Corridor

Drilling of the JT through the FLA significantly increased the surgical corridor between the CNs and foramina from 113.0 ± 11.6 mm^2 to 177.3 ± 30.6 mm^2 (mean difference 64.3 mm^2, 95% CI: 45.7-83.0, $P < .001$). The surgical corridor was also significantly larger by the FLA (177.3 ± 30.6 mm^2) than by the FMA (82.7 ± 12.4 mm^2, mean difference 94.6 mm^2, 95% CI: 71.1-118.8, $P < .001$). In addition, the CTM provided a greater corridor (212.2 ± 32.2 mm^2) than the FMA (mean difference 129.5 mm^2, 95% CI: 107.7-151.1, $P < .001$), with a clear trend toward greater exposure after CTM compared with FLA (mean difference 34.8 mm^2, 95% CI: −1.3 to 70.9, $P = .057$).

Overall Area of Exposure

A significantly greater area of exposure was observed after removing the JT by FLA (344.3 ± 76.6 mm^2 vs 410.7 ± 78.1 mm^2; mean difference 66.4 mm^2, 95% CI: 55.0-77.7, $P < 0.01$). The overall mean area of exposure was significantly larger with FLA (410.7 ± 78.1 mm^2) compared with FMA (270.7 ± 21.9 mm^2; mean difference 92.5 mm^2, 95% CI: 33.1-151.9, $P = .006$), but no significant difference was found between FLA and CTM (mean difference −26.1 mm^2, 95% CI: −86.6 to 34.3, $P = .3$).

Angle of Surgical Trajectory

The angle of trajectory to the JT was significantly greater ($P < .001$) for CTM (33.8° ± 7.1°) compared with FMA (14.3° ± 2.6°), as shown in Figure 5. The CTM increases the angle of the corridor by 19.5° (95% CI: 17.4-21.7, $P < .001$; Table).

Volumetric Assessment

The mean percentage of resection of the JT provided by each approach was 56.7% for FLA, 40.4% for FMA, and 94% for CTM (Figure 6). Using paired comparisons, CTM exceeded FLA by 36.9% (95% CI: 30.5-43.3, $P < .001$) and FMA by 53.2% (95% CI: 48.1-58.3, $P < .001$), whereas FLA exceeded FMA by 16.3% (95% CI: 10.2-22.5, $P < .001$).

Illustrative Cases

Case 1

A 45-year-old woman presented with hoarseness and dysphagia. MRI revealed an extradural lesion invading the left-sided JT and extending to the mastoid portion of the temporal bone. A left-sided far lateral transtubercular approach with an additional

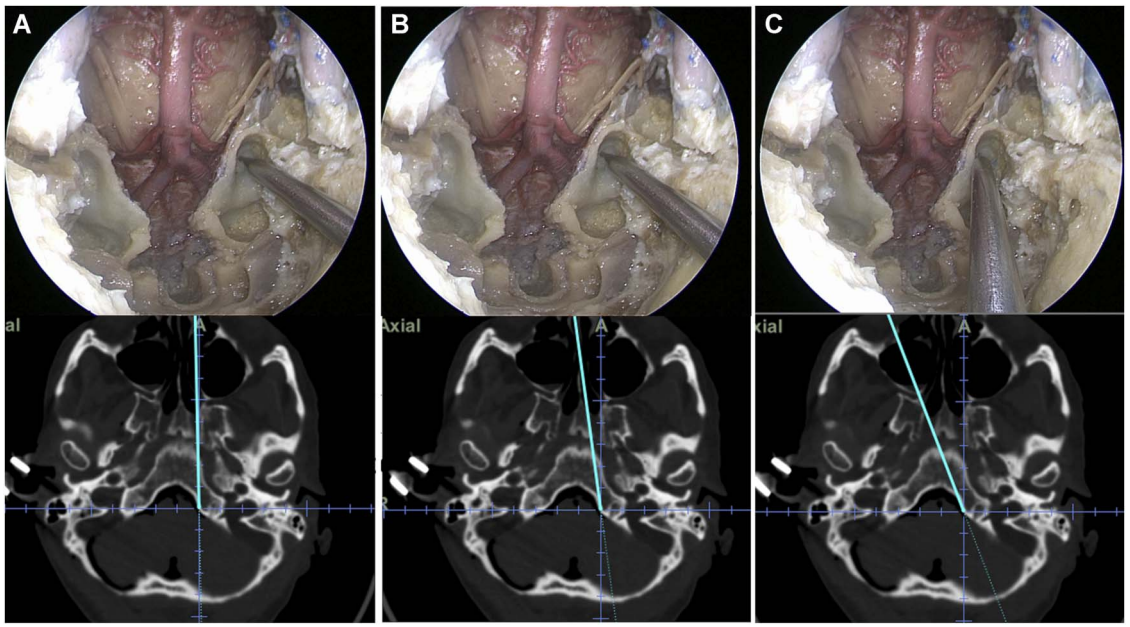

FIGURE 5. *Angle of surgical trajectory in relation with the JT.* **A**, *Cadaveric photograph showing the neuronavigation probe touching the left-sided JT as viewed from the left nostril, along with the corresponding CT-scan screenshot.* **B**, *Right-sided nostril.* **C**, *CTM approach. CT, computed tomography; CTM, contralateral transmaxillary; JT, jugular tubercle.*

mastoidectomy was performed to address the tumor's significant extradural component involving the JF (Figure 7). This provided optimal exposure for vascular control and lower CN preservation, enabling safe gross total resection of the pathology-confirmed paraganglioma. The postoperative course was uncomplicated.

TABLE. Measurements in Degrees of the Angle of Approach Relative to the JT

Specimen		Approach angle		
No.	**Side**	**EEA**	**CTM**	**Difference**
1	R	18.51	32.92	14.41
2	L	11.27	27.42	16.15
3	R	14.40	36.34	21.94
4	L	15.09	38.37	23.28
5	R	12.17	32.82	20.65
6	L	12.05	29.36	17.31
7	R	17.94	36.42	18.48
8	L	16.09	38.75	22.66
9	R	13.52	31.88	18.36
10	L	11.94	33.93	21.99
Mean		**14.30**	**33.82**	**19.52**

CTM, contralateral transmaxillary; EEA, endoscopic endonasal approach; L, left; JT, jugular tubercle, R, right.

Case 2

A 51-year-old woman presented with imbalance and dysphagia. Imaging revealed an extra-axial, homogeneous, and well-circumscribed lesion centered on the right-sided JT with a broad dural base (Figure 8), and an FMA was planned. After internal debulking and piecemeal extracapsular dissection, the tumor was completely removed, and the brainstem decompressed (Figure 8F). The postoperative course was uneventful, and pathology confirmed meningioma.

Case 3

A 63-year-old woman presented with progressive headache and diplopia. MRI revealed a high-intensity T2-weighted lesion at the skull base, involving the basilar part of the occipital bone and extending to the JT (Figure 9). The patient underwent a right-sided FMA, including extensive bone work and tumoral debulking. The inferior lateral clivus was identified, and the tumor, which had infiltrated the right JT bone, was resected. The postoperative course was uncomplicated, and pathology confirmed grade 2 chondrosarcoma.

Case 4

A 48-year-old woman presented with right-sided facial numbness and tingling with mild trigeminal dysfunction on

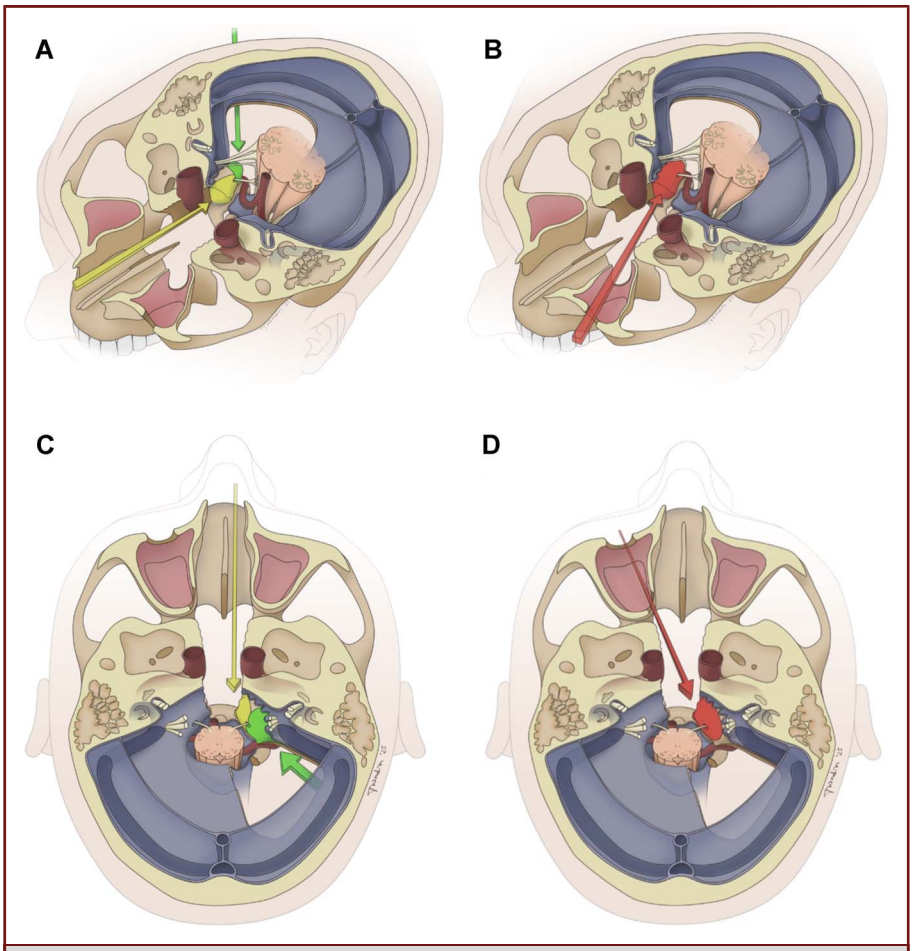

FIGURE 6. *Schematic images in oblique* **A** *and* **B**, *and axial* **C** *and* **D**, *views illustrating the area of interest of the JT resected after each approach, drawn based on the postdrilling CT scan. FMA (yellow arrow); FLA (green arrow); CTM (red arrow). CT, computed tomography; CTM, contralateral transmaxillary; FMA, far medial approach; FLA, far lateral approach; JT, jugular tubercle.*

examination. MRI revealed a large T2-hyperintense, gadolinium-enhancing lesion in the right petrous pyramid, petroclival junction, and basilar part of the occipital bone, extending into the middle cranial fossa, prepontine cistern, and cerebellopontine angle. The CT scan showed significant bone erosion, reaching the JT (Figure 10). The patient underwent a left CTM, along with an endoscopic transclival approach to the posterior cranial fossa and an endoscopic right transpterygoid approach to the middle cranial fossa. A gross total resection was achieved. The postoperative course was uneventful, pathology confirmed chondrosarcoma, and follow-up imaging showed complete resection with no recurrence.

Case 5

A 42-year-old woman presented with imbalance and right-sided facial numbness. The MRI showed a lesion with homogeneous enhancement, featuring a broad dural base and clear involvement of the right-sided IAC, extending inferiorly to the JT (Figure 11). A left CTM was performed in addition to an EEA. After extensive bone work, internal debulking, and precise extracapsular dissection, the tumor was successfully near totally removed. The postoperative course was uneventful, with pathology confirming a meningioma. The patient remains asymptomatic without tumor growth.

DISCUSSION

The JT is a smooth, paramedian osseous protuberance of the occipital bone, and its caudal part creates a shallow furrow above the course of the lower CNs.[3,23] Posteriorly, it is continuous with the inner surface of the occipital condyle and is located around 12 to 20 mm deep in relation with the lateral surface of the condyle.[3] This study offers a volumetric assessment of the JT drilled by 1

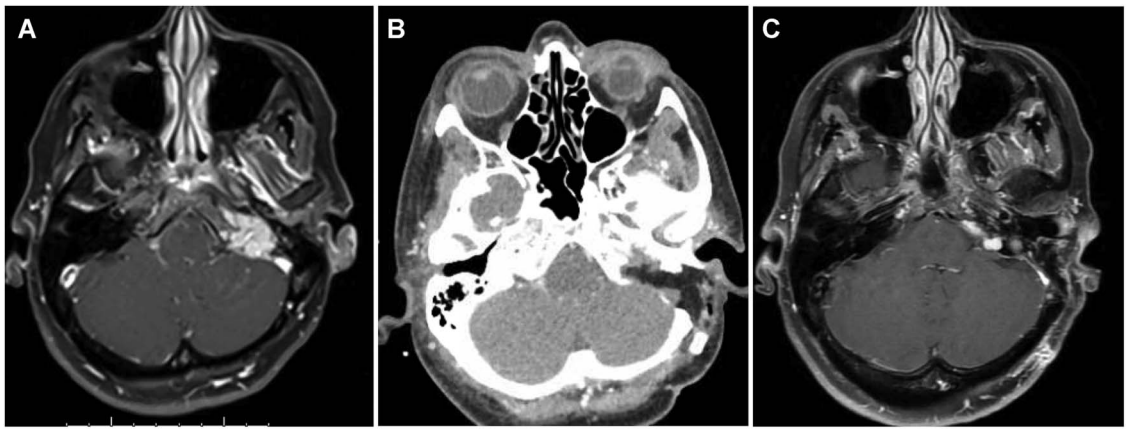

FIGURE 7. **A**, *Preoperative axial T1-weighted contrast-enhanced MRI demonstrating an extradural lesion involving the left-sided JT.* **B**, *Postoperative axial CT scan showing the bone removal through the FLA.* **C**, *Postoperative axial T1-weighted contrast-enhanced MR imaging showing gross total resection of the paraganglioma. CT, computed tomography; FLA, far lateral approach; JT, jugular tubercle.*

open and 2 endoscopic approaches, showing a relative advantage for the CTM.

To maximize surgical exposure with the FLA, adequate drilling of the JT is essential. Previous morphometric analysis of the JT showed that, quantitatively, surgical removal of this bone structure offers the most significant increase in the exposed petroclival area.[3] Without removing the JT, the views of the lower clivus, paramedullary area, VA, and vertebrobasilar junction would be obstructed. Drilling this structure significantly expands the operative field at the foramen magnum, extending toward the clivus and providing a flat, unobstructed view. Transcranial drilling of the JT is technically challenging because of the deep, narrow working space and proximity to the lower CNs, which are at risk from direct trauma, dural stretching, or heat. Its location near venous sinuses also makes venous bleeding common.

During the FLA, the dorsal superior- and medial-third of the condyle are drilled away until the hypoglossal canal is reached. Removal of the JT starts at the level of the hypoglossal canal in a posteroanterior direction toward the clivus and continues very deep for the entire length of the JT. Our study found that the narrow corridor between these structures restricts surgical access compared with the CTM.

The FLA provides a lateral-to-medial trajectory, whereas the FMA allows access to the JT through a medial-to-lateral route, offering a more direct course to this structure with the critical neural structures at the end point of access. In the ventromedial transjugular tubercle approach, the medial portion of the JT is drilled extradurally without manipulation of the lower CNs or mobilization of the sigmoid sinus, providing advantages over conventional open approaches that may reduce approach-related morbidity. This approach increases the lateral surgical corridor in the vertical axis, and when it is associated with condylar drilling, a significant vertical surgical window is opened. Once the JT is removed, direct visualization of the lower CNs just before their entry point into the JF is achieved.

Large clival chordomas and chondrosarcomas that extend laterally are difficult to manage purely endonasally. Among tumors that invade the lower clivus, Koutourousiou et al[6] reported that gross total resection was achieved in only 41.7% when tumor was extended to the JF and occipital condyle. The difficulty in approaching these more lateral and inferior clival/petroclival regions by an EEA occurs from the limited angle provided by the bony structure of the pyriform aperture, combined with the intricate anatomy of the foramen lacerum and Eustachian tube. Maneuvers such as releasing the pterygosphenoidal fissure and Eustachian tube, drilling the lingual process, and mobilizing the lacerum segment of the ICA can enhance access to the JT, but they also elevate procedural risks without substantially expanding lateral access. Patel et al[12] showed that the CTM enables an augmented endoscopic approach to the petrous apex, reaching lateral aspects that would not have been accessible by EEA or would require extensive dissection and mobilization of the ICA. In our study, we found that CTM increases the angle of the corridor to the JT by 19.5° when compared with the FMA.

Appropriate clinical examples are included, encompassing 1 case through FLA, 2 cases through FMA, and 2 cases through CTM. These cases focused on several pathologies: meningioma, chordoma, chondrosarcoma, and paraganglioma; importantly, only the latter pathology originated lateral to the lower CNs, rendering it best treated from a lateral approach. This is a key guiding principal in addition to the amount of JT access. A medial approach, such as FMA or CTM, is anatomically superior as it obviates the need for CN manipulation. Previous studies have indicated that the most common site for residual chordoma after EEA is inferior and lateral,[12,24] closer to the JT, and our study demonstrates that the CTM corridor enhances access to these areas.

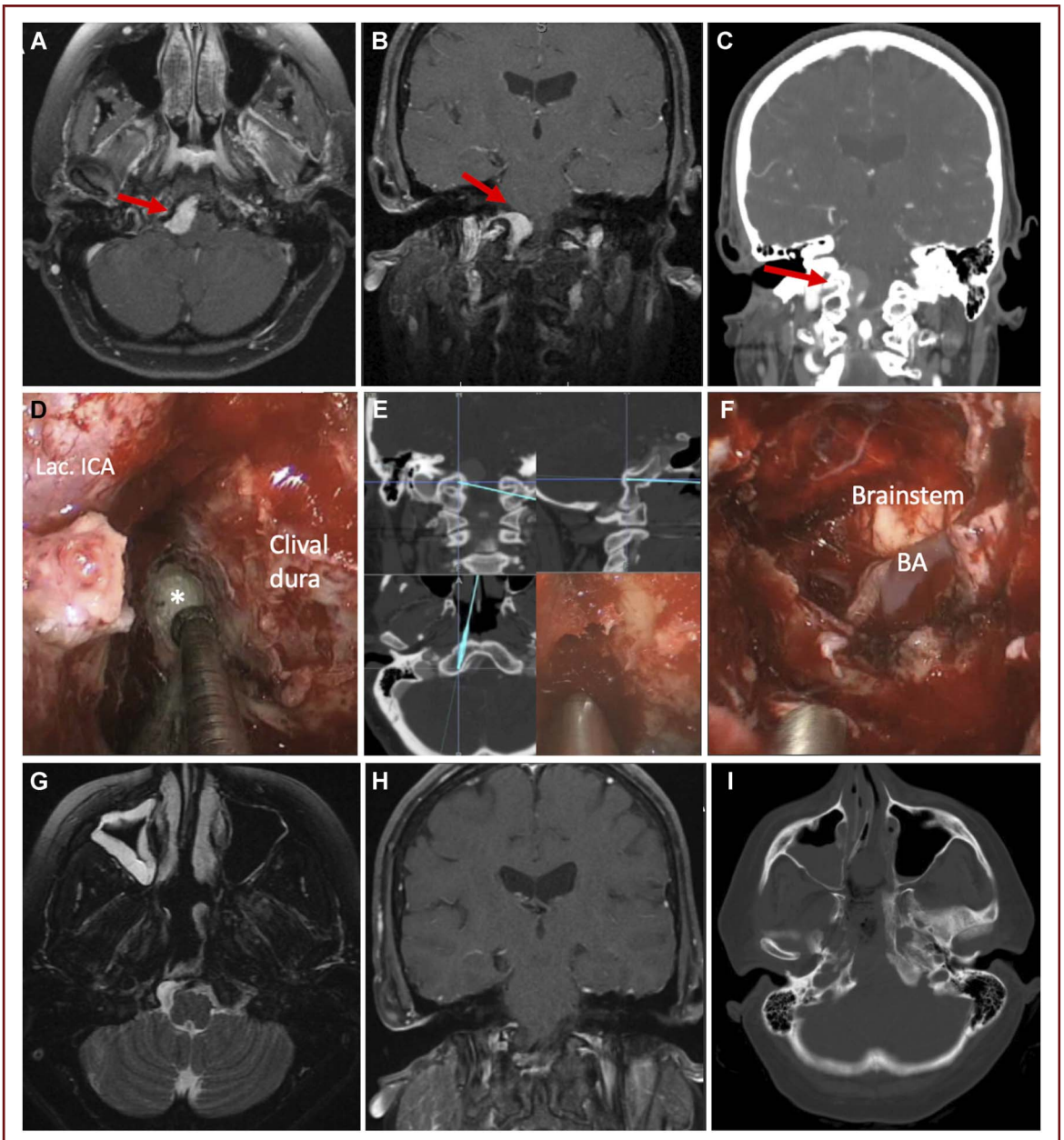

FIGURE 8. **A**, *Preoperative axial T1-weighted contrast-enhanced MRI revealing a right-sided JT meningioma with a broad dural base (arrow).* **B**, *Preoperative coronal T1-weighted image contrast-enhanced MRI illustrating the relationship of the lesion with the JT (arrow).* **C**, *Preoperative axial CT scan showing the relationship of the lesion with the hypoglossal canal (arrow).* **D**, *Intraoperative image from a far medial transtubercular approach, illustrating the drilling of the right JT (asterisk).* **E**, *Intraoperative neuronavigation images,* **F**, *Intradural anatomy after tumor resection, demonstrating brainstem decompression.* **G**, *Postoperative axial T2-weighted MRI showing complete resection of the meningioma.* **H**, *Postoperative coronal T1-weighted MRI showing brainstem decompression.* **I**, *Postoperative axial CT scan exhibiting the extension of bone removal. BA, basilar artery; Lac., lacerum segment; ICA; internal carotid artery; JT, jugular tubercle.*

Limitations

A limitation of this study is the reliance on indirect volumetric measurements obtained through neuronavigation for certain variables, which may not fully represent surgical exposure in a clinical setting.

CONCLUSION

Open and endonasal approaches are complementary for lesions in the inferior clival/petroclival region. The CTM

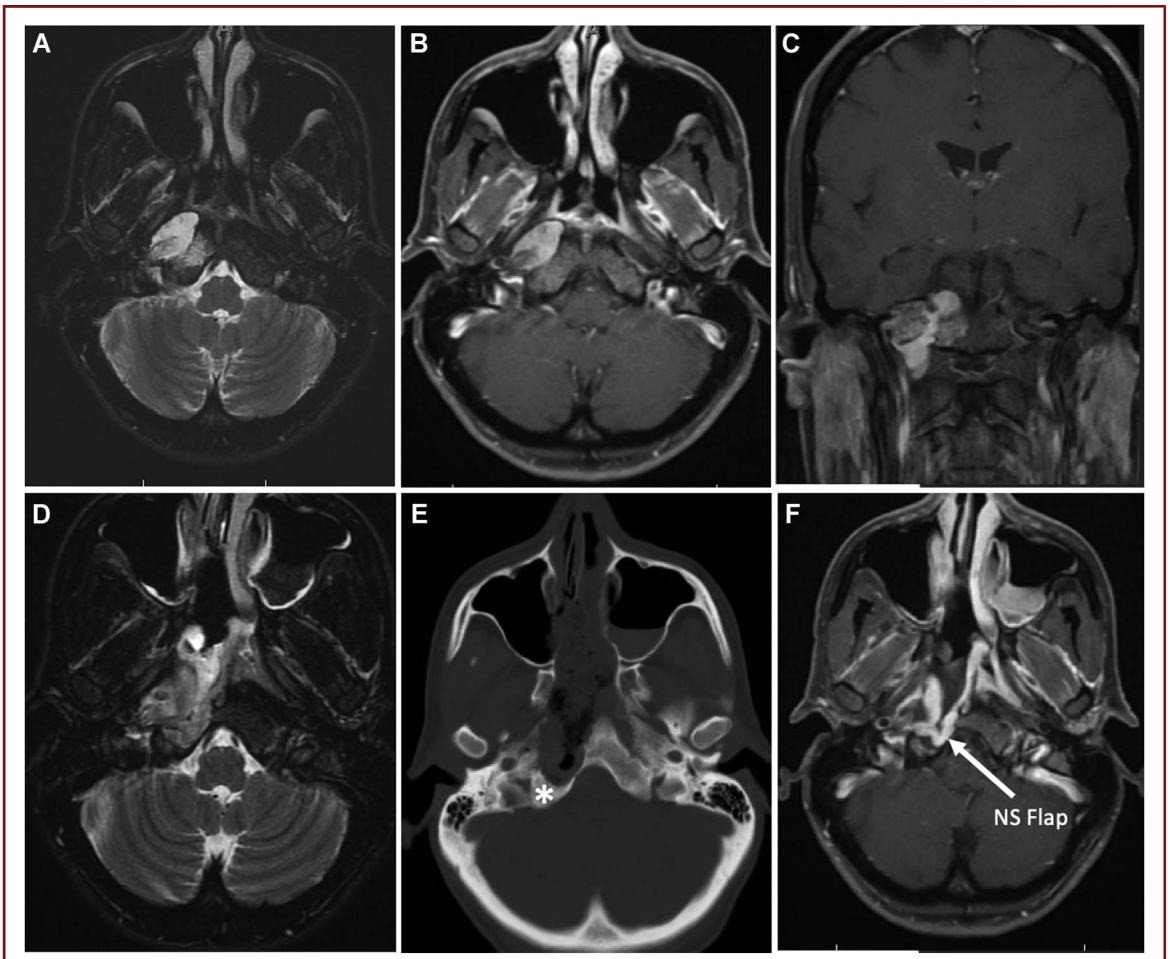

FIGURE 9. **A**, *Preoperative axial T2-weighted MRI showing a high-intensity lesion involving the basilar part of the occipital.* **B**, *Preoperative axial T1-weighted contrast-enhanced MRI displaying a right-sided chondrosarcoma of the skull base.* **C**, *Preoperative coronal T1-weighted contrast-enhanced MRI demonstrating partial involvement of the JT.* **D**, *Postoperative axial T2-weighted MRI.* **E**, *CT scan confirming the removal of the infiltrated bone of the JT (asterisk highlighting the residual normal JT).* **F**, *Postoperative axial T1-weighted contrast-enhanced MRI demonstrating gross total resection and the NS flap used for reconstruction (white arrow). CT, computed tomography; JT, jugular tubercle; NS, nasoseptal.*

functions as a feasible extension of the standard EEA, widening the surgical corridor angle and providing greater JT exposure than the FMA. It also allows significantly greater JT removal compared with both the FLA and FMA, making it the preferred approach for bony lesions involving the JT.

Funding

This study did not receive any funding or financial support.

Disclosures

The authors have no personal, financial, or institutional interest in any of the drugs, materials, or devices described in this article.

REFERENCES

1. Fernandez-Miranda JC, Morera VA, Snyderman CH, Gardner P. Endoscopic endonasal transclival approach to the jugular tubercle. *Neurosurgery.* 2012;71(1 suppl operative):146-159.
2. Funaki T, Matsushima T, Peris-Celda M, Valentine RJ, Joo W, Rhoton AL. Focal transnasal approach to the upper, middle, and lower clivus. *Neurosurgery.* 2013; 73(2 suppl operative):155-191.
3. Mintelis A, Sameshima T, Bulsara KR, Gray L, Friedman AH, Fukushima T. Jugular tubercle: morphometric analysis and surgical significance. *J Neurosurg.* 2006;105(5):753-757.
4. Wen HT, Rhoton AL, Katsuta T, De Oliveira E. Microsurgical anatomy of the transcondylar, supracondylar, and paracondylar extensions of the far-lateral approach. *J Neurosurg.* 1997;87(4):555-585.
5. Matsushima T, Natori Y, Katsuta T, Ikezaki K, Fukui M, Rhoton AL. Microsurgical anatomy for lateral approaches to the foramen magnum with special reference to transcondylar fossa (supracondylar transjugular tubercle) approach. *Skull Base Surg.* 1998;8(3):119-125.

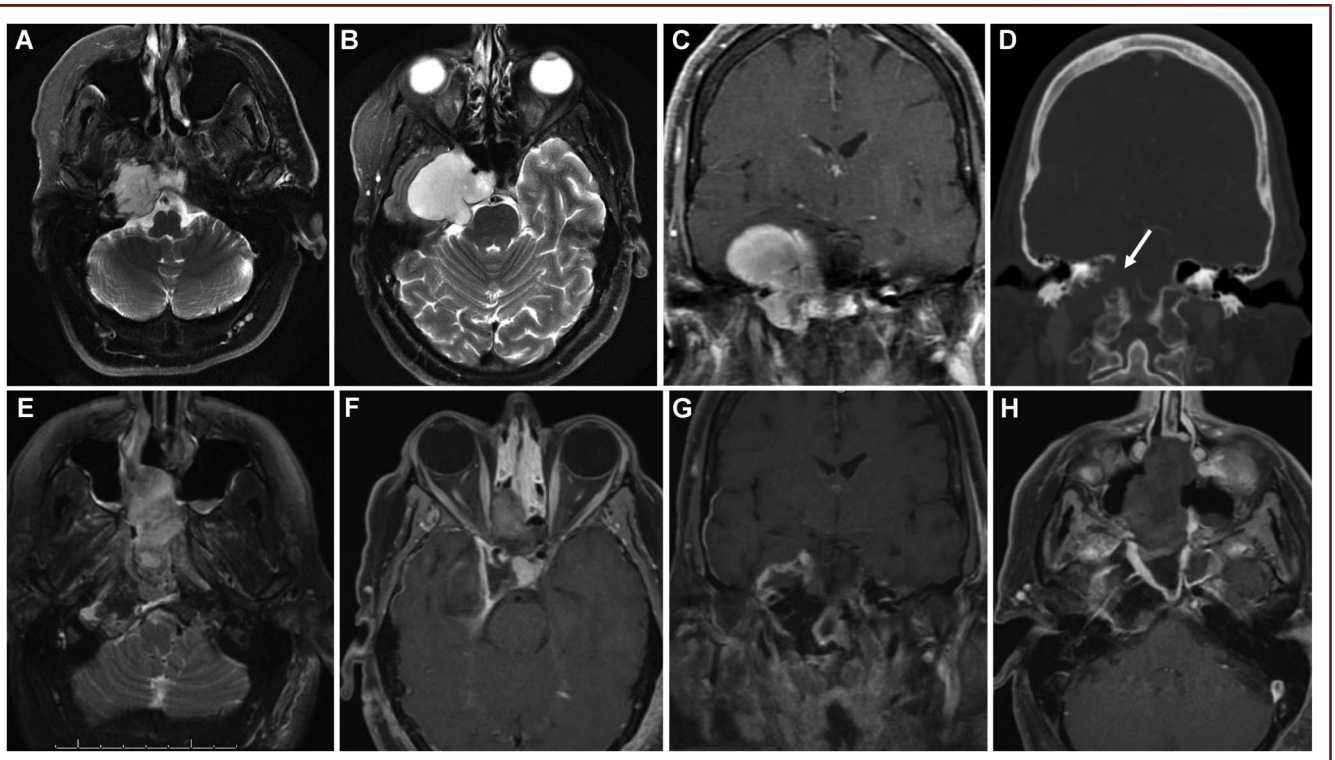

FIGURE 10. *Preoperative images demonstrating a large lesion in the skull base:* **A** *and* **B**, *axial T2-weighted MRI.* **C**, *Coronal T1-weighted contrast-enhanced MRI.* **D**, *Axial CT scan demonstrating erosion of the right JT (white arrow). Postoperative images demonstrating a gross total resection of the chondrosarcoma:* **E**, *axial T2-weighted MRI.* **F**, *Axial T1-weighted contrast-enhanced MRI highlighting the resection of the middle fossa component.* **G**, *Coronal T1-weighted contrast-enhanced MRI.* **H**, *Axial T1-weighted contrast-enhanced MRI exhibiting the NS flap used for reconstruction. CT, computed tomography; NS, nasoseptal; JT, jugular tubercle.*

6. Koutourousiou M, Gardner PA, Tormenti MJ, et al. Endoscopic endonasal approach for resection of cranial base chordomas: outcomes and learning curve. *Neurosurgery.* 2012;71(3):614-625.
7. Taniguchi M, Kohmura E. Endoscopic endonasal removal of laterally extended clival chordoma using side-viewing scopes. *Acta Neurochir.* 2012;154(4):627-632.
8. Saito K, Toda M, Tomita T, Ogawa K, Yoshida K. Surgical results of an endoscopic endonasal approach for clival chordomas. *Acta Neurochir.* 2012;154(5):879-886.
9. Stippler M, Gardner PA, Snyderman CH, Carrau RL, Prevedello DM, Kassam AB. Endoscopic endonasal approach for clival chordomas. *Neurosurgery.* 2009;64(2):268-278.
10. Vaz-Guimaraes Filho F, Wang EW, Snyderman CH, Gardner PA, Fernandez-Miranda JC. Endoscopic endonasal "far-medial" transclival approach: surgical anatomy and technique. *Oper Tech Otolaryngol Head Neck Surg.* 2013;24(4):222-228.
11. Morera VA, Fernandez-Miranda JC, Prevedello DM, et al. "Far-medical" expanded endonasal approach to the inferior third of the clivus: the transcondylar and transjugular tubercle approaches. *Neurosurgery.* 2010;66(6 suppl operative):211-220.
12. Patel CR, Wang EW, Fernandez-Miranda JC, Gardner PA, Snyderman CH. Contralateral transmaxillary corridor: an augmented endoscopic approach to the petrous apex. *J Neurosurg.* 2018;129(1):211-219.
13. Lang DA, Neil-Dwyer G, Iannotti F. The suboccipital transcondylar approach to the clivus and cranio-cervical junction for ventrally placed pathology at and above the foramen magnum. *Acta Neurochir.* 1993;125(1-4):132-137.
14. Spektor S, Anderson GJ, McMenomey SO, Horgan MA, Kellogg JX, Delashaw JB. Quantitative description of the far-lateral transcondylar transtubercular approach to the foramen magnum and clivus. *J Neurosurg.* 2000;92(5):824-831.
15. Nanda A, Vincent DA, Vannemreddy PSSV, Baskaya MK, Chanda A. Far-lateral approach to intradural lesions of the foramen magnum without resection of the occipital condyle. *J Neurosurg.* 2002;96(2):302-309.
16. Baldwin HZ, Miller CG, Van Loveren HR, Keller JT, Daspit CP, Spetzler RF. The far lateral/combined supra- and infratentorial approach. A human cadaveric prosection model for routes of access to the petroclival region and ventral brain stem. *J Neurosurg.* 1994;81(1):60-68.
17. Kratimenos GP, Crockard HA. The far lateral approach for ventrally placed foramen magnum and upper cervical spine tumours. *Br J Neurosurg.* 1993;7(2):129-140.
18. Benet A, Prevedello DM, Carrau RL, et al. Comparative analysis of the transcranial "far lateral" and endoscopic endonasal "far medial" approaches: surgical anatomy and clinical illustration. *World Neurosurg.* 2014;81(2):385-396.
19. Dean NR, Illing EA, Woodworth BA. Endoscopic resection of anterolateral maxillary sinus inverted papillomas. *Laryngoscope.* 2015;125(4):807-812.
20. Lee JT, Suh JD, Carrau RL, Chu MW, Chiu AG. Endoscopic Denker's approach for resection of lesions involving the anteroinferior maxillary sinus and infratemporal fossa. *Laryngoscope.* 2017;127(3):556-560.
21. Seiberling K, Ooi E, MiinYip J, Wormald PJ. Canine fossa trephine for the severely diseased maxillary sinus. *Am J Rhinol Allergy.* 2009;23(6):615-618.
22. Upadhyay S, Dolci RLL, Buohliqah L, Prevedello DM, Otto BA, Carrau RL. Endoscopic endonasal anterior maxillotomy. *Laryngoscope.* 2015;125(12):2668-2671.
23. Karam YR, Menezes AH, Traynelis VC. Posterolateral approaches to the craniovertebral junction. *Neurosurgery.* 2010;66(3 suppl):135-140.
24. Van Rompaey J, Arturo Solares C. Transmaxillary approach to the infratemporal fossa. *Oper Tech Otolaryngol Head Neck Surg.* 2013;24(4):218-221.

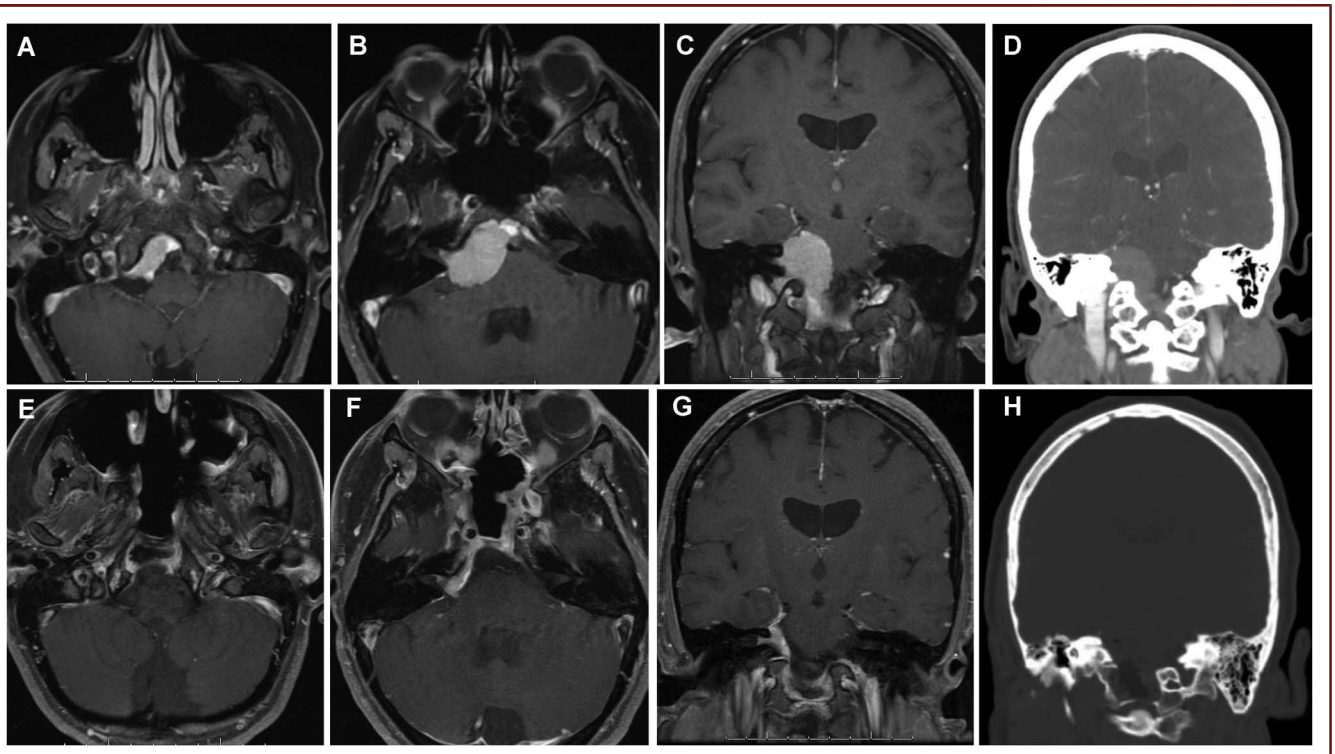

FIGURE 11. *Preoperative MRI:* **A** *and* **B**, *axial T1-weighted contrast-enhanced MRI.* **C**, *Coronal T1-weighted contrast-enhanced MRI.* **D**, *Coronal CT scan demonstrating right-sided JT involvement. Postoperative images demonstrating a near total resection of the meningioma:* **E** *and* **F**, *axial T1-weighted contrast-enhanced MRI.* **G**, *Coronal T1-weighted contrast-enhanced MRI.* **H**, *Coronal CT scan showing the resection of the right-sided JT. CT, computed tomography; JT, jugular tubercle.*

Acknowledgements

Author contribution: C.F.: methodology, data collection, investigation, data analysis, writing—original draft, review and editing; A.P.: data collection, data analysis, writing—review and editing; Y-.K.C.: data collection, data analysis, writing—review and editing; A.T.: data analysis, writing—review and editing; G.A.Z.: methodology, data analysis, writing—review and editing; E.W.W.: methodology, data analysis, writing—review and editing; C.H.S.: composition, methodology, data analysis, writing—review and editing; P.A.G.: composition, methodology, data analysis, writing—review and editing.

Supplemental digital content *is available for this article at operativeneurosurgery-online.com.*

Supplemental digital content 1, Figure 1: Stereotactic measurements of the surgical corridor. Far lateral approach before (A) and after (B) drilling of the jugular tubercle; endoscopic endonasal far medial approach (C) and contralateral transmaxillary corridor (D). We considered the following landmarks: (a) caudal-most aspect of IX rootlet (superomedial), (b) medial tip of the JT [predrilling] and entry point of IX nerve [postdrilling] (superolateral), (c) cranial-most aspect of XII rootlet (inferomedial), (d) cranial-most entry point of XII nerve into the hypoglossal canal (inferolateral), and (e) IAC (extreme superior and lateral point).

Supplemental digital content 2, Figure 2: Stereotactic measurements of the area of exposure. Ventral view through the far lateral approach (A) and dorsal view through endoscopic approaches (B). Dorsally, we considered the following landmarks: (a) obex (superomedial), (b) dural entry point of IX nerve (superolateral), (c) dorsal median sulcus at the C1 level (inferomedial), (d) dural entry point of the cranial-most aspect of C1 rootlet (inferolateral), and (e) IAC (extreme superior and lateral point). Ventrally: (a) pontomedullary junction (superomedial), (b) entry point of IX on JF (superolateral), (c) ventral median sulcus at C1 level (inferomedial), (d) condyle (inferolateral), and (e) IAC (extreme superior and lateral point).

COMMENTS

Access to the jugular tubercle (JT) remains one of the defining challenges in skull base surgery, given its deep location and intimate relationship with several critical neurovascular structures. The authors present a rigorous quantitative comparison of the far lateral (FLA), far medial (FMA), and contralateral transmaxillary (CTM) approaches, integrating cadaveric dissection, stereotactic measurements, volumetric analyses, and illustrative cases to advance our understanding of this anatomically complex region.

The key contribution of this study is the demonstration that the CTM corridor meaningfully expands the surgical angle, corridor width, and volumetric resection of the JT while maintaining the advantages of an endoscopic endonasal approach, namely limiting the need for CN manipulation or extensive bony removal. In particular, the CTM offers a powerful solution for medially based lesions with lateral extension toward the foramen magnum, providing access that historically required condylar drilling and/or transposition of

neurovascular structures. These findings underscore the evolving paradigm where extended endoscopic endonasal routes increasingly complement, rather than replace, open transcranial approaches, likewise celebrating the value in utilizing multidisciplinary skull base teams.

Importantly, the authors also contextualize their anatomical data with clinical illustrations that further highlight when open, endonasal, or combined strategies are most appropriate. The distinction between lesions arising lateral vs medial to the lower CNs remains a critical determinant of surgical planning, and this study provides the quantitative framework to guide these decisions.

Future work should focus on correlating these anatomical advantages with clinical outcomes, including extent of resection, complication profiles, and reconstructive considerations.

Nonetheless, this study establishes a foundational framework for integrating CTM into the surgical armamentarium for complex lesions of the inferior clival and petroclival skull base.

The authors are commended for their meticulous methodology and for providing data that bridge anatomical precision with clinical relevance in one of the most challenging regions of the cranial base.

Danielle Dang and Maria Peris Celda
Rochester, Minnesota, USA